This article has been accepted for inclusion in a future issue of this journal. Content is final as presented, with the exception of pagination.

Abnormal Odor Detection in Electronic Nose via Self-Expression Inspired Extreme Learning Machine

Lei Zhang, *Member, IEEE*, and Pingling Deng

Abstract*—The electronic nose (E-nose), as a metal oxide semiconductor gas sensor system coupled with pattern recognition algorithms, is developed for approximating artificial olfaction functions. Ideal gas sensors should be with selectivity, reliability, and cross-sensitivity to different odors. However, a new problem is that abnormal odors (e.g., perfume, alcohol, etc.) would show strong sensor response, such that they deteriorate the usual usage of E-nose for target odor analysis. An intuitive idea is to recognize abnormal odors and remove them online. A known truth is that the kinds of abnormal odors are countless in real-world scenarios. Therefore, general pattern classification algorithms lose effect because it is expensive and unrealistic to obtain all kinds of abnormal odors data. In this paper, we propose two simple yet effective methods for abnormal odor (outlier) detection: 1) a self-expression model (SEM) with l_1/l_2-norm regularizer is proposed, which is trained on target odor data for coding and then a very few abnormal odor data is used as prior knowledge for threshold learning and 2) inspired by self-expression mechanism, an extreme learning machine (ELM) based self-expression (SE^{2}LM) is proposed, which inherits the advantages of ELM in solving a single hidden layer feed-forward neural network. Experiments on several datasets by an E-nose system fabricated in our laboratory prove that the proposed SEM and SE^{2}LM methods are significantly effective for real-time abnormal odor detection.

***Index Terms*—Electronic nose (E-nose), extreme learning machine (ELM), odor detection, self-expression.**

I. Introduction

DURING the past two decades, the electronic nose (E-nose) as a kind of artificial olfaction system, has been explored in depth from the viewpoints of applications, systems and algorithms. Artificial olfaction system constructed by a model nose was originally proposed to mimic biological olfactory mechanism in 1982 [1]. The definition of artificial olfaction was further validated by Gardner and Bartlett [2], who claimed that an E-nose was an instrument comprising of an array of chemical sensors with partial specificity and a pattern recognition system, for recognizing simple or complex odors.

Manuscript received October 24, 2016; revised February 1, 2017 and March 14, 2017; accepted March 30, 2017. This work was supported in part by the National Natural Science Foundation of China under Grant 61401048 and Grant 61471073, and in part by the Research Fund Project of Central Universities. This paper was recommended by Associate Editor H. Ying. *(Corresponding author: Lei Zhang.)*

The authors are with the College of Communication Engineering, Chongqing University, Chongqing 400044, China (e-mail: leizhang@cqu.edu.cn; dengpl@cqu.edu.cn).

Color versions of one or more of the figures in this paper are available online at http://ieeexplore.ieee.org.

Digital Object Identifier 10.1109/TSMC.2017.2691909

A. Background

Gas sensor technology and artificial intelligence are the research foundation of artificial olfaction systems (i.e., an E-nose). An E-nose has been widely applied in a number of applications, such as food/beverage quality control (e.g., milk analysis, tea analysis, meal analysis, etc.) [3]–[5], environmental monitoring (e.g., gas analysis, air quality monitoring, etc.) [6]–[10], medical diagnosis (e.g., diabetes analysis, cancer analysis, etc.) [11]–[13], and public safety monitoring (e.g., tobacco, explosive, etc.) [14], [15]. So far, a number of E-nose systems have been developed by researchers with different kinds of sensors [16], implementation strategies [17], [18], and hardware platform [19]. In our previous work [9], the E-nose system and experimental setup for odor data collection have been presented. In this paper, we aim at solving the abnormal odor disturbance detection in this community based on the proposed E-nose system.

Currently, there are commonly three challenging problems in the E-nose community, which are summarized as 3-D (i.e., discreteness, drift, and disturbance) issue in [20]. Specifically, the discreteness issue has been well handled in recent years by using calibration transfer methods [21]–[24]. The drift issue is currently a hot problem in E-noses, which is recognized to be time-varying noise and difficult to be described by some deterministic models. A number of different methods have been proposed by researchers to compensate and process the drift [25]–[29], and big progress has been achieved by using transfer learning techniques. However, for the disturbance issue (i.e., abnormal odors), there is little work in E-noses [30], [31], [45]. Specifically, Zhang *et al.* [30] and Phaisangittisagul and Nagle [45] followed a general classification route and simply take abnormal odors as one class, but neglect that there are thousands of abnormal odors which are impossible to collect. Tian *et al.* [31] attempted to establish a self-correspondence by using a regression idea, i.e., predicting one sensor by using other sensors based on the target samples, but neglect the intrinsic independence between sensors. This disturbance issue is closely related to the cross-sensitivity characteristics of gas sensors. Generally speaking, during the

This article has been accepted for inclusion in a future issue of this journal. Content is final as presented, with the exception of pagination.

target gases sensing by an E-nose system, the gas sensors show strong response when exposed to the disturbances (abnormal odors, e.g., perfume, alcohol, etc.). Consequently, the sensors are seriously deteriorated and the target odor detection by an E-nose comes to a failure in such application scenarios. In this paper, we would focus on the abnormal odor detection and improve the E-nose performance in complex application scenarios (i.e., with abnormal odors).

B. Problem Statement

As claimed above, we target at solving the disturbance (i.e., abnormal odors) problem in E-nose. An intuitive idea is to recognize the abnormal odors, because the abnormal odors are with large intervariance by comparing to target odors (i.e., normal odors) that are detected by an E-nose of the same type. With this idea, it may not be difficult to have a rational strategy based on appropriate pattern recognition algorithms to train a model for classification, by treating abnormal odors as one class and target odors as another class. However, we have to face with the fact that there are so many kinds of disturbances (countless) appeared in real-world air scenarios, such that the discrimination between target odors and abnormal odors cannot be simply recognized as a general pattern recognition problem, because it is expensive and unrealistic to acquire all kinds of abnormal odor data. Therefore, abnormal odor detection without "seeing" some prior knowledge of abnormal odor patterns is currently an open and urgent problem to be solved.

C. Motivation

By thinking about the above problem from scratch, we get that, in our E-nose system, although the prior knowledge of abnormal odor detection is deficient, the prior knowledge of target odor data (six kinds of contaminants) can be easily obtained. Therefore, the problem becomes how to accurately detect the abnormal odors by using the data of target odors. Our motivations are as follows.

1) For abnormal odor detection, the prior knowledge of target odor can be recognized as some invariant information, which is used for modeling some self-correspondence. Once the established self-correspondence when feed into some input is violated, it will be categorized as abnormal odors.
2) To establish a self-correspondence, the prior knowledge of target odors may be modeled by using self-expression based on representation-based learning theory.
3) A fast learning algorithm for solving a single-hidden layer feed-forward neural network (SLFN), known as an extreme learning machine (ELM) proposed by Huang *et al.* [32], [33], has turned out to be the remedy for biological learning. ELM is with rather simple structure, and its speed can be thousands of times faster than the traditional network learning algorithms. Recently, ELM has been explored efficiently in hierarchal learning [34], transfer learning [35], and deep learning [36]. A deep insight of ELM theory about its learning mechanism and biological learning idea can be found in [37] and [38].

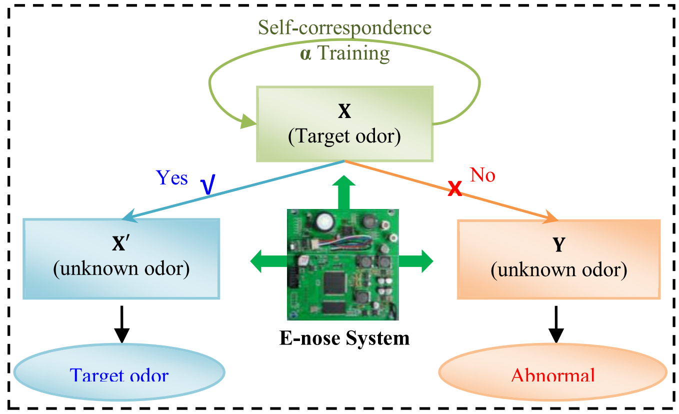

Fig. 1. Schematic of abnormal odor detection in our E-nose system. "Yes" indicates that the unknown odor $\mathbf{X}'$ complies with the self-correspondence $\boldsymbol{\alpha}$. "No" indicates that the unknown odor $\mathbf{Y}$ violates the self-correspondence. The odor data acquisition and detection is implemented in our E-nose system.

Inspired by self-expression and ELM, we would like to model the self-correspondence of target odor data as an SLFN network with nonlinear activation.

With the above motivations, the research on abnormal odor detection in an E-nose system by using self-expression learning and ELM is expanded. The idea and motivation can be briefly described in Fig. 1, which clearly shows the abnormality detection process by an E-nose system. Some other interesting applications in vision and tactile perception can be referred to as [39]–[43].

D. Paper Contribution

In this paper, we propose two methods including self-expression model (SEM) and ELM-based self-expression (SE^{2}LM), for abnormal odor detection in E-nose. The contributions of this paper are summarized as threefold.

1) We propose a self-correspondence concept based on the prior knowledge of target odors for abnormal odor detection, without using the prior information of abnormal odors in model training.
2) With the representation-based learning mechanism, an SEM with l_1/l_2-norm regularization is proposed in our E-nose system.
3) Inspired by biological learning concept of ELM, a heuristic self-expression method (SE^{2}LM) is proposed in our biological olfaction (E-nose) system for abnormal odor detection.

The basic idea of self-correspondence is illustrated in Fig. 1, which is simply divided into two steps. First, the training is conducted for self-correspondence establishment, and the coefficient $\boldsymbol{\alpha}$ describes the self-correspondence. Second, for abnormality detection, each new pattern is represented by using the self-correspondence coefficient matrix, and representation error is computed for abnormality detection. As shown in Fig. 2, in testing phase, the instances $\mathbf{y}_1$, $\mathbf{y}_2$, and $\mathbf{y}_3$ indicate target odor, therefore small errors are observed. However, the instance $\mathbf{y}_4$ indicates abnormal odor, and a big error is observed, that is used to recognize the abnormal odor based on error criteria.

This article has been accepted for inclusion in a future issue of this journal. Content is final as presented, with the exception of pagination.

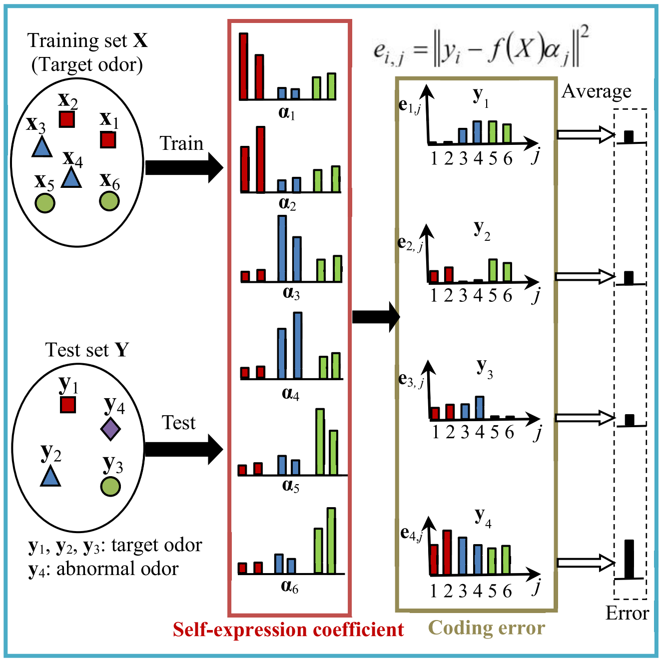

Fig. 2. Framework of the self-correspondence mechanism. Both SEM and SE^{2}LM are proposed based on this framework. In the training data X (target odor data), six samples of three target classes are shown for obtaining the self-correspondence coefficients ($\boldsymbol{\alpha}_1, \ldots, \boldsymbol{\alpha}_6$). In the testing data Y, four samples of three target classes and one abnormal class are used to calculate the coding error ($\mathbf{e}_1, \ldots, \mathbf{e}_4$).

E. Paper Organization

This rest of this paper is organized as follows. Section II illustrates the related work closely related with this paper. Section III presents the proposed SEM framework including model formulation and algorithm. The proposed SE^{2}LM framework is presented in Section IV. The E-nose experiments on several datasets for abnormal odor detection are conducted in Section V. A brief discussion about the violation threshold and model parameter is presented in Section VI. Finally, Section VII concludes this paper.

F. Notations

In this paper, the training phase consists of two parts: first, compute the self-expression matrix $\boldsymbol{\alpha}$ and second, determine the violation threshold T (representation error). $\mathbf{X} \in \Re^{D\times N}$ is the target odor data used for computing the coding coefficient matrix $\boldsymbol{\alpha}$. The training data of a very few abnormal odor data is denoted as $\mathbf{Y} \in \Re^{D\times n}$ ($n \ll N$), respectively, where D is the number of dimensions, N and n are the number of training samples, and $\boldsymbol{\alpha}$ is the self-expression coding coefficient matrix. $\|\cdot\|_F$ denotes Frobenius norm of a matrix. $\|\cdot\|_1$ denotes l_1-norm, and $\|\cdot\|_2$ denotes l_2-norm. $\mathrm{Tr}(\cdot)$ denotes the trace operator. Throughout this paper, matrix is written in capital bold face, vector is presented in lower bold face, and variable is in italics.

II. Related Works

ELM [32] is closely related with this paper, and therefore presented in this section. The magic of ELM is that the parameters of weight and bias can be assigned randomly independent of training data, and do not require computationally intensive tuning upon the data. Besides, the output weights can be solved with different constraints. The activation function can be any type of piecewise continuous nonlinear hidden neurons, such as sigmoid function, Fourier function, RBF function, etc. In learning process, the hidden layer nodes (number of neurons) can be tuned in terms of the actual situation, which naturally do not require an iterative adjustment. ELM has been successfully applied for handling regression and classification problems. Briefly, the principle of ELM [32] for generalized SLFNs is described as follows.

In the case of clean data, the output of ELM is presented as

$$f(\mathbf{x}) = \sum_{i=1}^{L} \boldsymbol{\beta}_i G(\mathbf{a}_i, b_i, \mathbf{x}) \tag{1}$$

where $\mathbf{x}$ is the input vector, L is the number of hidden nodes, $\mathbf{a}_i$ is the input weights, b_i is the bias of the hidden nodes, and $\boldsymbol{\beta}_i$ is the output weights between the ith hidden node and the output nodes. $f(\mathbf{x})$ is the corresponding target output vectors and $G(\mathbf{a}_i, \mathrm{b}_i, \mathbf{x})$ is the output vector of the ith hidden neuron. Equation (1) can also be compactly written as

$$f(\mathbf{x}) = \mathbf{h}(\mathbf{x})\boldsymbol{\beta} \tag{2}$$

where $h_i(\mathbf{x}) = \mathrm{G}(\mathbf{a}_i, \mathrm{b}_i, \mathbf{x})$ is the output vector of the ith hidden neuron, thus $\mathbf{h}(\mathbf{x}) = [h_1(\mathbf{x}), h_2(\mathbf{x}), \ldots, h_L(\mathbf{x})]$ is the output matrix of the hidden layer and $\boldsymbol{\beta} = [\boldsymbol{\beta}_1, \boldsymbol{\beta}_2, \ldots, \boldsymbol{\beta}_L]$ is the output weights matrix. In order to minimize the norm of the output weights, the minimal norm least square constraint is used in ELM, such that a closed-form solution can be obtained, instead of the standard gradient descent-based optimization methods. Thus, the output weights $\boldsymbol{\beta}$ can be determined analytically using Moore–Penrose (MP) generalized inverse as

$$\boldsymbol{\beta} = \mathbf{h}(\mathbf{x})^{+}\mathbf{T} \tag{3}$$

where $\mathbf{T}$ is the label hypothesis and $\mathbf{h}(\mathbf{x})^{+}$ is the MP generalized pseudo-inverse of the hidden layer output matrix. $\boldsymbol{\beta}$ has the smallest norm among all the optimization solutions, and this is the reason why ELM has better generalization performance and higher learning accuracy. According to Bartlett's neural network generalization theory, in addition to achieving smaller training error, the smaller the norms of weights are, the better generalization performance of the networks tend to be. The regularized ELM is expressed as

$$\min_{\boldsymbol{\beta}} \|\boldsymbol{\beta}\|_F^2 + C\|\mathbf{H}\boldsymbol{\beta} - \mathbf{T}\|_F^2. \tag{4}$$

Then the solution can be written as

$$\boldsymbol{\beta} = \mathbf{H}^{\mathrm{T}}\left(\frac{\mathbf{I}}{C} + \mathbf{H}\mathbf{H}^{\mathrm{T}}\right)^{-1}\mathbf{T}, \text{ if } N \le L \tag{5}$$

where N is the number of training samples, and L is the number of hidden nodes.

When the number of training samples N is larger than that of nodes L, then one can have

$$\boldsymbol{\beta} = \left(\frac{\mathbf{I}}{C} + \mathbf{H}^{\mathrm{T}}\mathbf{H}\right)^{-1}\mathbf{H}^{\mathrm{T}}\mathbf{T}, \text{ if } N > L \tag{6}$$

where $\mathbf{I}$ is an identity matrix.

This article has been accepted for inclusion in a future issue of this journal. Content is final as presented, with the exception of pagination.

III. Proposed Self-Expression Model for Abnormality Detection

A. Framework Formulation

There are numerous types of abnormal odors in real-world application scenarios, which can seriously deteriorate the performance of E-nose systems. Obviously, it is expensive and unrealistic for researchers to obtain all of them in experiments as training samples. Therefore, we attempt to use the prior information of the target odors for modeling the self-correspondence. Specifically, the prior knowledge of target odors is invariant information, and thus for constructing a self-correspondence model, it is rational to imagine that an SEM can be designed for capturing the internal relationship (i.e., self-correspondence) among target odors. The relationship within target odors can be used to detect the abnormality if "violation" of this relationship is encountered. The proposed SEM method includes two phases: 1) self-correspondence learning and 2) violation threshold learning.

1) Self-Correspondence $\boldsymbol{\alpha}$ Learning: Instinctively, the relationship can be modeled by satisfying

$$\mathbf{X} = \mathbf{X}\alpha \tag{7}$$

where $\boldsymbol{\alpha} \in \Re^{N\times N}$ describes the self-correspondence and $\mathbf{X} \in \Re^{D\times N}$ denotes the training set of target odors. It is important to find a robust $\boldsymbol{\alpha}$ based on (7). Generally, we propose to solve $\boldsymbol{\alpha}$ by minimizing the following objective:

$$\min_{\boldsymbol{\alpha},\boldsymbol{\alpha}_{ii}=0,\ \forall i} \|\mathbf{X}-\mathbf{X}\boldsymbol{\alpha}\|_F^2 + \lambda \cdot R(\boldsymbol{\alpha}) \tag{8}$$

where $0 < \lambda \leq 1$ denotes the regularization coefficient, and $R(\boldsymbol{\alpha})$ represents an appropriate regularizer formulated as

$$R(\boldsymbol{\alpha}) = \|\boldsymbol{\alpha}\|_p \tag{9}$$

where $\|\cdot\|_p$ indicates l_p-norm. Specifically, $p = 1$ denotes sparsity constraint is imposed on $\boldsymbol{\alpha}$, and $p = 2$ shows better smoothness of the self-correspondence. Therefore, with $p = 1$, the SEM-sparse model is formulated as follows:

$$\min_{\boldsymbol{\alpha},\boldsymbol{\alpha}_{ii}=0,\ \forall i} \|\mathbf{X}-\mathbf{X}\boldsymbol{\alpha}\|_F^2 + \lambda \cdot \|\boldsymbol{\alpha}\|_1. \tag{10}$$

With $p = 2$, the SEM-smooth model is formulated as follows:

$$\min_{\boldsymbol{\alpha},\boldsymbol{\alpha}_{ii}=0,\ \forall i} \|\mathbf{X}-\mathbf{X}\boldsymbol{\alpha}\|_F^2 + \lambda \cdot \|\boldsymbol{\alpha}\|_F^2. \tag{11}$$

2) Violation Threshold T Learning: After obtaining the self-correspondence $\boldsymbol{\alpha}$, the coding error E_X of target odor pattern $\mathbf{x}$ is calculated as

$$E_X(\mathbf{x}_j) = \frac{1}{N}\sum_{i=1}^{N}\|\mathbf{x}_j - \mathbf{X}\boldsymbol{\alpha}_i\|^2, j = 1,\cdots,N. \tag{12}$$

Similarly, the coding error E_Y of abnormal odor pattern $\mathbf{y}$ is

$$E_Y(\mathbf{y}_j) = \frac{1}{N}\sum_{i=1}^{N}\|\mathbf{y}_j - \mathbf{X}\boldsymbol{\alpha}_i\|^2, j = 1,\ldots,n. \tag{13}$$

The violation threshold T can be determined by uniform search between the minimum E_X (i.e., $E_{X,\min}$) and the maximum E_X (i.e., $E_{X,\max}$), until the average classification accuracy of $\mathbf{X}$ and $\mathbf{Y}$ is maximized. Then, the optimal T is determined as

$$T^* = \mathop{\arg\max}_{E_{X,\min}\leq T\leq E_{X,\max}} \frac{1}{2}(\text{Accuracy}(X) + \text{Accuracy}(Y)). \tag{14}$$

Note that for simplification, the target odors are categorized as one class (i.e., normal class). The classification accuracy is easy to be computed by using the popular coding error. Additionally, other strategies other than the average accuracy can also be used in (14) for determining the threshold. Once the optimal T is determined, the abnormal odor detection can be made by comparing T^* with the coding error E_z computed in (12) or (13) when given a new instance z. Without loss of generality, if $E_z \geq T^*$, then z is discriminated as some kind of abnormal odor. Otherwise, z is recognized to be one kind of target odors.

Algorithm 1: SEM (SEM-Sparse Versus SEM-Smooth)

Input:
The training data $\mathbf{X} \in \mathbb{R}^{D\times N}$ and $\mathbf{Y} \in \mathbb{R}^{D\times n}$;
Parameter λ;
Procedure:
• *Phase 1: self-correspondence* $\boldsymbol{\alpha}$ *learning*
if l_1-norm constraint is used (p=1), solve Eq.(10) by using *Lasso* operator (SEM-sparse)
  for $i, j = 1$ *to* N
    Initialize $\alpha_{i,j} = \mathbf{x}_j^{\mathrm{T}}\mathbf{x}_i$;
    Update $\alpha_{i,j}$ by using Eq.(15);
  end
else if l_2-norm constraint is used (p=2), solve Eq.(11) by using *least-square* operator (SEM-smooth)
  Compute the close-form solution $\boldsymbol{\alpha}$ by using Eq.(16);
• *Phase 2: violation threshold T learning*
  Compute E_{X} and E_{Y} using Eq.(12) and (13);
  Compute the optimal T^* by solving Eq.(14).
Output: $\boldsymbol{\alpha}$ and T^*.

B. Algorithm

According to the SEM framework, two steps in training phase are included as follows.

For the first step, two models in (10) and (11) are presented based on l_1/l_2-norm regularizer.

When l_1-norm constraint on $\boldsymbol{\alpha}$ is considered, (10) is a sparse optimization problem, and can be easily solved by a standard *Lasso* solver [44]. Generally, the update strategy of $\alpha_{i,j}$ is shown as

$$\alpha_{i,j} = \text{sign}(\alpha_{i,j})\left(|\alpha_{i,j}| - \frac{\lambda}{2}\right)_+ \tag{15}$$

where $(|\alpha_{i,j}| - (\lambda/2))_+ = \max(|\alpha_{i,j}| - (\lambda/2), 0)$.

When l_1-norm constraint on $\boldsymbol{\alpha}$ is considered, (11) is a least-square optimization problem, and a closed-form solution can be induced as follows:

$$\boldsymbol{\alpha} = \left(\mathbf{X}^{\mathrm{T}}\mathbf{X} + \lambda\cdot\mathbf{I}\right)^{-1}\mathbf{X}^{\mathrm{T}}\mathbf{X}. \tag{16}$$

Specifically, the detailed implementation of the whole SEM framework for abnormality detection (abnormal odor) is summarized as Algorithm 1.

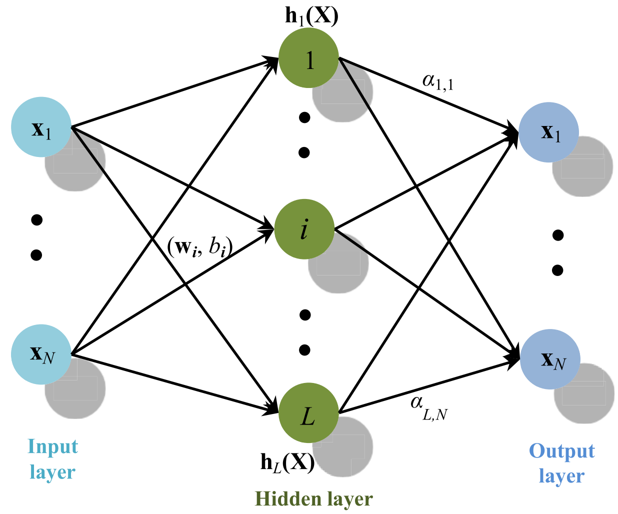

Fig. 3. Network structure of SE^{2}LM. The difference between this structure and ELM lies in that the number of input nodes is associated with the dimensionality. In SE^{2}LM, it serves for representing each sample by using hidden layer output and the analytically determined output weights $\boldsymbol{\alpha}$. It implies that the ELM space represents the dictionary space. Note that an interesting aspect is that in ELM, the number of input nodes and output nodes can be the dimension D, which would become a transformation problem. If N is set, it is expression problem focused in this paper. Also, in the proposed structure, each node is composed of D subnodes (i.e., shadow nodes).

IV. Proposed Extreme Learning Machine-Based Self-Expression Model

A. Model Formulation

In (7), the self-expression is purely linear. Inspired by ELM theory, we propose to establish the self-correspondence by using the nonlinearity activated data in SE^{2}LM space (i.e., hidden layer output). Suppose the random hidden layer output of SE^{2}LM to be $\mathbf{H} \in \Re^{D\times L}$, then (7) can be further written as

$$\mathbf{X} = \mathbf{H}\boldsymbol{\alpha} \tag{17}$$

where $\boldsymbol{\alpha} \in \Re^{L\times N}$ denotes the output weights between hidden layer and output layer, and $\mathbf{H}$ is represented as follows:

$$\mathbf{H} = \begin{bmatrix} h(\mathbf{w}_1\mathbf{x}_1 + b_1) & h(\mathbf{w}_2\mathbf{x}_1 + b_2) & \cdots & h(\mathbf{w}_L\mathbf{x}_1 + b_L) \\ h(\mathbf{w}_1\mathbf{x}_2 + b_1) & h(\mathbf{w}_2\mathbf{x}_2 + b_2) & \cdots & h(\mathbf{w}_L\mathbf{x}_2 + b_L) \\ \vdots & \vdots & \vdots & \vdots \\ h(\mathbf{w}_1\mathbf{x}_D + b_1) & h(\mathbf{w}_2\mathbf{x}_D + b_2) & \cdots & h(\mathbf{w}_L\mathbf{x}_D + b_L) \end{bmatrix} \tag{18}$$

where $h(\cdot)$ indicates the activation function, such as sigmoid, Gaussian function, etc., L denotes the number of hidden nodes, $\mathbf{W} = [\mathbf{w}_1, \ldots, \mathbf{w}_L] \in \Re^{N\times L}$ is the randomly generated weights between input layer and hidden layer, and $\mathbf{B} = [b_1, \ldots, b_L]^{\mathrm{T}} \in \Re^{L}$ is the randomly generated bias for hidden nodes.

The structure of SE^{2}LM is shown in Fig. 3, which is similar with ELM yet different in nodes design for self-expression.

Specifically, the proposed SE^{2}LM model is formulated as

$$\begin{aligned} &\min_{\boldsymbol{\alpha},\boldsymbol{\xi}_i,\forall i} \ \frac{1}{2}\|\boldsymbol{\alpha}\|_F^2 + \frac{1}{2}\mu\cdot\sum_{i=1}^{N}\left\|\boldsymbol{\xi}_i\right\|^2 \\ &\text{s.t.} \quad \boldsymbol{\xi}_i = \mathbf{x}_i - \mathbf{H}\boldsymbol{\alpha}_i, i = 1, \ldots, N. \end{aligned} \tag{19}$$

Algorithm 2: SE^{2}LM

Input:
The training data $\mathbf{X} \in \mathbb{R}^{D\times N}$ and $\mathbf{Y} \in \mathbb{R}^{D\times n}$;
Parameter μ;
Procedure:
- *Phase 1: self-correspondence* $\boldsymbol{\alpha}$ *learning*
  Generate the input weights $\mathbf{W}$ and hidden bias $\mathbf{B}$ randomly;
  Compute the hidden layer matrix $\mathbf{H}$ by using Eq.(18);
  Compute the output weights $\boldsymbol{\alpha}$ by using Eq.(21);
- *Phase 2: violation threshold T learning*
  Compute E_{X} and E_{Y} using Eq.(22) and (23);
  Compute the optimal T^* by solving Eq.(14).

Output: $\boldsymbol{\alpha}$ and T^*.

The model in (19) can be compactly written as

$$\begin{aligned} &\min_{\boldsymbol{\alpha},\boldsymbol{\xi}} \ \frac{1}{2}\|\boldsymbol{\alpha}\|_F^2 + \frac{1}{2}\mu\cdot\|\boldsymbol{\xi}\|_F^2 \\ &\text{s.t.} \quad \boldsymbol{\xi} = \mathbf{X} - \mathbf{H}\boldsymbol{\alpha}. \end{aligned} \tag{20}$$

The model can also be explained as that each sample can be represented by the dictionary $\mathbf{H}$ through the coefficient $\boldsymbol{\alpha}$. Additionally, the proposed SE^{2}LM inherits the advantages of ELMs. The objective is to learn the self-correspondence coefficients $\boldsymbol{\alpha}$, based on the fixed dictionary $\mathbf{H}$. That is, the SE^{2}LM is only proposed in training process.

B. Algorithm

Similar to SEM framework, in SE^{2}LM framework, the same two phases are included.

1) Self-Correspondence $\boldsymbol{\alpha}$ *Learning:* The optimization of SE^{2}LM model (20) can be easily conducted, by following similar induction with ELM. Specifically, the closed-form solution of $\boldsymbol{\alpha}$ can be described as follows:

$$\boldsymbol{\alpha} = \begin{cases} \mathbf{H}^{\mathrm{T}}\left(\frac{\mathbf{I}}{\mu} + \mathbf{H}\mathbf{H}^{\mathrm{T}}\right)^{-1}\mathbf{X}, & \text{if } D \le L \\ \left(\frac{\mathbf{I}}{\mu} + \mathbf{H}^{\mathrm{T}}\mathbf{H}\right)^{-1}\mathbf{H}^{\mathrm{T}}\mathbf{X}, & \text{if } D > L. \end{cases} \tag{21}$$

The deduction of (21) is similar to the standard ELM framework, by considering the property of hidden matrix $\mathbf{H}$.

2) Violation Threshold T Learning: After obtaining the self-correspondence $\boldsymbol{\alpha}$, similar to (12) and (13), the coding error E_X of target odor pattern $\mathbf{x}$ is calculated as

$$E_X(\mathbf{x}_j) = \frac{1}{N}\sum_{i=1}^{N}\left\|\mathbf{x}_j - \mathbf{H}\boldsymbol{\alpha}_i\right\|^2, j = 1, \ldots, N. \tag{22}$$

Similarly, the coding error E_Y of abnormal odor pattern $\mathbf{y}$ is

$$E_Y(\mathbf{y}_j) = \frac{1}{N}\sum_{i=1}^{N}\left\|\mathbf{y}_j - \mathbf{H}\boldsymbol{\alpha}_i\right\|^2, j = 1, \ldots, n. \tag{23}$$

The search process of the optimal T is similar to (14).

Specifically, the whole process for abnormality detection of SE^{2}LM framework is summarized as Algorithm 2.

V. E-Nose Experiments for Abnormal Odor Detection

Our E-nose system and experimental setup developed in this paper have been described previously in [9]. The E-nose system is composed of an array of metal oxide semiconductor sensors, which includes TGS2602, TGS2620, TGS2201A, and TGS2201B. Additionally, the gas sensors are also sensitive to the environmental variables, such as temperature and humidity, and result in an impact on concentration measure and discrimination of gases. Therefore, a module of temperature and humidity (i.e., STD2230-I2C), which is used to measure the ambient temperature and humidity, is also integrated in our E-nose system. The real-time response of this module has been used as feature variables in our algorithms for environmental compensation. In this paper, six kinds of target odors/gases including formaldehyde (HCHO), benzene (C_6H_6), toluene (C_7H_8), carbon monoxide (CO), ammonia (NH_3), and nitrogen dioxide (NO_2) are being detected by our E-nose.

That is, other odors except the six target odors will be uniformly categorized as abnormal odors. In addition to computing the recognition accuracy, we also collect two extra real-time sequences for validating the effectiveness of the proposed frameworks in real-time application scenarios. The data acquisition experiments were measured in a gas chamber, where the E-nose system was fixed. The odor sample (target odor and abnormal odor) mixed with pure nitrogen (i.e., N_2) is collected in a gas bag, and an air pump is used to transfer the odor from the bag to the chamber, controlled by a flowmeter for different concentrations. During the measurements, the temperature and relative humidity of the gas chamber are set within 10 °C–40 °C and 40%–80% RH.

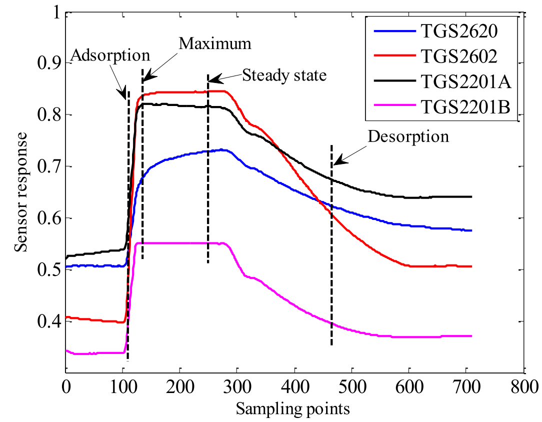

Fig. 4. Sensor response curves for each observation. Four important phases of sensor response mechanism are highlighted. The steady state point for each sensor is extracted as feature of each observation.

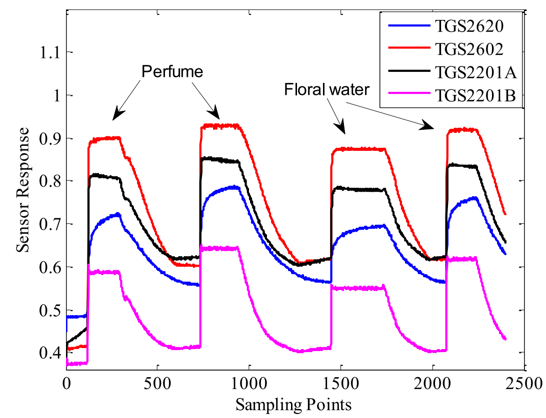

Fig. 5. Real-time sensor response sequence when exposed to abnormal odors such as perfume and floral water. A peak response will be produced when abnormal odors exist.

A. Experimental Data

In this paper, three benchmark datasets that have been used for abnormal odor detection in [20], [30], and [31] are used for verifying our proposed methods.

1) Dataset 1 (Pretraining and Test of the Proposed Framework): This dataset 1 was collected by using an E-nose system when exposed to the six kinds of targets odors. We aim to learn the self-correspondence coefficients $\boldsymbol{\alpha}$ and the violation error threshold T by using the proposed SEM and SE^{2}LM frameworks based on dataset 1 with six kinds of target gases: 1) HCHO; 2) C_6H_6; 3) C_7H_8; 4) CO; 5) NH_3; and 6) NO_2. In experiments, the number of target samples for HCHO, C_6H_6, C_7H_8, CO, NH_3, and NO_2 are 188, 72, 66, 58, 60, and 38, respectively. Each sample can be represented as four curves in Fig. 4, where the steady state point is extracted as feature of each observation (sample). In self-expression, the whole target odor dataset 1 is divided into three parts: 1) the data for training $\boldsymbol{\alpha}$; 2) the data for training T; and 3) the test data. The detail of target odor data is illustrated in Table I, in which the proportionality for each part is shown. Additionally, 48 samples of alcohol (abnormal odor) were also used. The alcohol dataset is divided into two parts: 1) 24 samples for training T and 2) 24 samples for testing. This dataset 1 is used for model training and validation. The detection accuracy of target odor and abnormal odor is reported based on this dataset (i.e., 96 target samples and 24 abnormal samples).

2) Dataset 2 (Real-Time Abnormal Odor Without Target Odor): For validating the effectiveness of the proposed frameworks, we choose some common abnormal odors in our life and do a real-time experiment. The dataset 2 was collected based on the same E-nose system, by exposing E-nose to abnormal odors, such as perfume, floral water, and fruits smell. Note that, these abnormal odors do not participate in $\boldsymbol{\alpha}$ training. Specifically, an observation vector with length of 2400 points for each sensor was acquired in a continuous sampling way. This dataset was developed under two odor interferences in order, i.e., perfume and floral water. In detail, we present the approximation positions for each odor as follows. Perfume appears in two approximated regions 95–308 and 709–958; floral water appears in two approximated regions 1429–1765 and 2056–2265. Visually, the sensor sequences of dataset 2 are illustrated in Fig. 5.

3) Dataset 3 (Real-Time Abnormal Odor With Target Odor): Dataset 3 is also a real-time data sequence for validation. Dataset 3 was obtained by exposing the same E-nose system to abnormal odor and one kind of target odor (HCHO), simultaneously. Similar to dataset 2, dataset 3 is with length of

This article has been accepted for inclusion in a future issue of this journal. Content is final as presented, with the exception of pagination.

TABLE I
TARGET ODOR SAMPLES (DATASET 1) FOR MODEL TRAINING AND TESTING

Target gases	formaldehyde	benzene	toluene	CO	NO_2	NH_3	Total
Number of Total Samples	188	72	66	58	38	60	482
Number of samples for training $\boldsymbol{\alpha}$	75	29	27	23	15	24	193
Number of samples for training T	75	29	27	23	15	24	193
Number of test samples	38	14	12	12	8	12	96

TABLE II
RECOGNITION ACCURACY (%) OF ABNORMAL ODOR DETECTION UNDER DIFFERENT NUMBER OF TRAINING SAMPLES PER CLASS FOR TRAINING $\boldsymbol{\alpha}$

Number of samples per class		40	35	30	25	20	15	10
SEM-sparse (l_1-norm)	Target odor	98.99	98.99	87.88	59.6	52.53	17.17	0
	Abnormal odor	75	75	91.67	100	100	100	100
	Average	*87*	*87*	***89.78***	*79.8*	*76.27*	*58.59*	*50*
SEM-smooth (l_2-norm)	Target odor	98.99	96.97	77.78	48.48	3.03	2.51	0
	Abnormal odor	50	58.33	91.67	100	100	100	100
	Average	*74.5*	*77.65*	***84.73***	*74.24*	*51.52*	*51.75*	*50*
SE^2LM (Sigmoid)	Target odor	100	92.93	90.91	80.81	72.73	34.34	15.15
	Abnormal odor	66.67	83.33	91.67	100	100	100	100
	Average	*83.34*	*88.13*	***91.29***	*90.4*	*86.37*	*67.17*	*57.57*
SE^2LM (Gaussian)	Target odor	100	91.92	90.91	76.77	57.58	52.53	5.05
	Abnormal odor	66.67	83.33	91.67	100	10	100	100
	Average	*83.34*	*87.63*	***91.29***	*88.39*	*78.77*	*76.27*	*52.53*

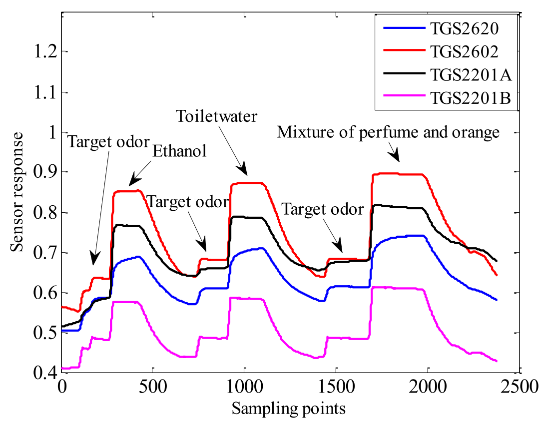

Fig. 6. Real-time sensor sequence exposed to target odor (HCHO) and abnormal odors such as ethanol, toiletwater, mixture of perfume, and orange.

2400 points for each sensor and acquired in a continuous sampling way. Specifically, this dataset is developed under HCHO (target odor) and four kinds of abnormal odors (disturbance), respectively. Briefly, HCHO appears in three approximated regions 102–250, 719–880, and 1380–1580; ethanol appears in region 260–410; floral water appears in region 881–1064; and a mixture of perfume and orange appears in region 1599–1899. Visually, the sensor sequences in dataset 3 are illustrated in Fig. 6.

B. Abnormal Odor Detection Based on Dataset 1

The training performance of the proposed SEM and SE^2LM frameworks is relevant to the data amount during training of $\boldsymbol{\alpha}$ and T. In experiments, to observe the performance impact with respect to the number of training samples in training $\boldsymbol{\alpha}$, 10, 15, 20, 25, 30, 35, and 40 samples per class in the training set are explored for sample balance, respectively. Due to the number of samples for some target odor shown in Table I is less than the maximum value (i.e., 40), we repeat the sample selection randomly for sample balance. The recognition accuracy is shown in Table II. For SE^2LM method, sigmoid function and Gaussian (RBF) function are used as activation function separately. From the results, we can see the best average performance when 30 samples per class are used in training set. The recognition accuracy of target odors is 90.91% and the accuracy of abnormal odors is 91.67%. Note that, we show the average performance, because in (14) the average accuracy is used as criteria in searching the optimal violation error threshold T. Additionally, we could observe that SE^2LM method outperforms SEM method for different settings. The SEM with sparse l_1-norm constraint achieves 89.78%, which is much better than SEM with smooth l_2-norm constraint (84.73%). This demonstrates that the self-correspondence coefficients $\boldsymbol{\alpha}$ should be sparse for robust self-expression.

Similarly, for observing the impact with respect to the number of training samples in searching T, 10, 15, 20, 25, 30, 35, and 40 training samples per class in training set $\mathbf{X}$ are explored, respectively. The recognition accuracies are shown in Table III. We can observe that the best average accuracy is 91.29% when 25 samples per class are used. Also, it turns out to be that SE^2LM not only outperforms SEM but also show better stability when fewer training samples are used. Additionally, SEM-based methods show imbalanced recognition between target odor and abnormal odor. Specifically, we have shown the performance variation curves with respect to the threshold T in searching process as Fig. 7. We can observe that with the increasing of T, the recognition rate of target odor is decreasing due to that the rejection rate of target odor is increasing. In contrast, the recognition rate of abnormal odor is increasing. Clearly, the near-optimal T appears in their cross point region. From Fig. 7, the SE^2LM-based method shows better detection performance and lower bias for both target and abnormal odor. Note that the scale of T may be different which depends on the method. Also, the model parameters λ

TABLE III
RECOGNITION ACCURACY (%) OF ABNORMAL ODOR DETECTION UNDER DIFFERENT NUMBER OF TRAINING SAMPLES PER CLASS FOR TRAINING **T**

Number of samples per class		40	35	30	25	20	15	10
SEM-sparse (l_1-norm)	Target odor	98.99	98.99	78.79	75.76	74.75	94.95	98.99
	Abnormal odor	41.67	41.67	100	100	100	83.33	50
	Average	*70.33*	*70.33*	***89.4***	*87.88*	*87.38*	*89.14*	*74.5*
SEM-smooth (l_2-norm)	Target odor	85.86	89.9	51.52	79.8	94.95	86.42	74.75
	Abnormal odor	91.67	83.33	100	100	58.33	56.83	50
	Average	*88.77*	*86.62*	*75.76*	***89.9***	*76.64*	*71.63*	*62.38*
SE^{2}LM (Sigmoid)	Target odor	81.82	81.82	89.9	90.91	81.82	81.82	80.81
	Abnormal odor	100	100	91.67	91.67	100	100	100
	Average	*90.91*	*90.91*	*90.79*	***91.29***	*90.91*	*90.91*	*90.41*
SE^{2}LM (Gaussian)	Target odor	81.82	81.82	85.86	80.81	81.82	80.81	80.81
	Abnormal odor	100	100	100	100	100	100	100
	Average	*90.91*	*90.91*	***92.93***	*90.41*	*90.91*	*90.41*	*90.41*

TABLE IV
DETECTION ACCURACY (%) FOR DIFFERENT METHODS

Number of samples per class		ELM (sigmoid)	ELM (Gaussian)	PMIE (TGS2602)	PMIE (TGS2620)	PMIE (TGS2201A)	PMIE (TGS2201B)	SEM-sparse (l_1-norm)	SEM-smooth (l_2-norm)	SE^{2}LM (Sigmoid)	SE^{2}LM (Gaussian)
10	Target odor	89.08	84.67	82.42	85.93	68.88	74.72	98.99	74.75	80.81	80.81
	Abnormal odor	84.8	82.86	86.71	88	58.33	81.19	50	50	100	100
	Average	86.94	83.77	84.57	86.97	63.61	77.96	*74.5*	*62.38*	*90.41*	***90.41***
20	Target odor	79.3	77.45	85.93	86.34	92.12	78.34	74.75	94.95	81.82	81.82
	Abnormal odor	62.52	62.47	88.26	92.88	66.67	75	100	58.33	100	100
	Average	70.91	69.96	87.10	89.61	79.39	76.67	*87.38*	*76.64*	*90.91*	***90.91***
30	Target odor	40.84	52.84	87.14	87.37	75.55	84.27	78.79	51.52	89.9	85.86
	Abnormal odor	35.58	37.6	89.0	94.12	81.67	66.67	100	100	91.67	100
	Average	38.21	45.22	88.07	90.75	78.61	75.47	*89.4*	*75.76*	*90.79*	***92.93***

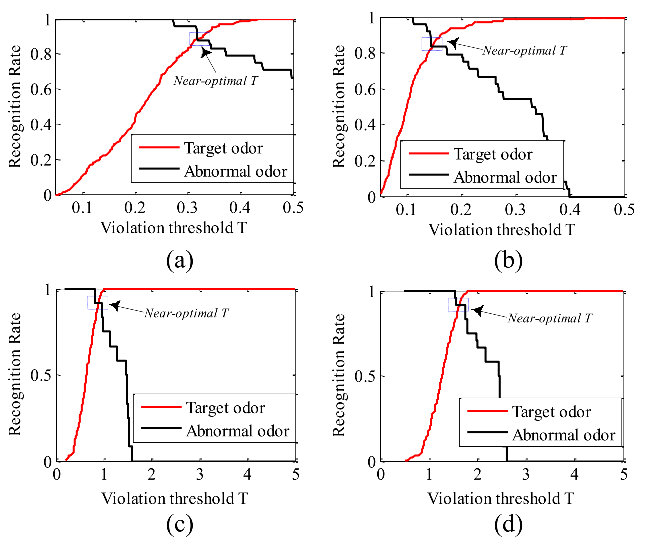

Fig. 7. Performance variation with respect to the violation threshold T for target and abnormal odor. The near-optimal T is labeled in rectangle region (the cross point). (a) SEM-sparse. (b) SEM-smooth. (c) SE^{2}LM (sigmoid). (d) SE^{2}LM (Gaussian).

and μ are tuned in the range of 10^{-4} and 10^{4}. For different tasks, the optimal model parameters may be different during the learning process.

Through the comparisons shown in Tables II and III, we can observe that the results based on SE^{2}LM are better than that of SEM-based methods. Generally, if we simply treat the target/abnormal odor recognition as a binary classification problem, the recognition accuracy by using conventional ELM classifier is shown in Table IV. Note that ELM (sigmoid) denotes the ELM classifier based on sigmoid kernel function. The principle of pattern mismatch-based interference elimination (PMIE) [31] is that a similar but different self-correspondence is established by regression between sensors based on target odor data, which is based on a regression idea. Specifically, PMIE uses five sensors to predict the remaining sensor for target odors, and search an optimal prediction error threshold. As shown in Table IV, we can observe that the results with general binary classification method between target odor (positive class) and abnormal odors (negative class) are much worse than the proposed SEM and SE^{2}LM methods. Besides, binary classification-based method should rely on all kinds of abnormal odors in real-world scenarios, which is expensive and unrealistic in E-nose. Therefore, both results and reality demonstrate that abnormal odor detection cannot be simply recognized as a binary classification problem. The truth also confirms the difficulty of problem and significance of our proposed methods. As shown in Table IV, the proposed SE^{2}LM method still outperforms other binary classification-based abnormal odors detection methods.

C. Validation on Real-Time Sequence Based on Dataset 2

As expressed in experimental data (i.e., dataset 2), this dataset was collected in real time and used for validating the proposed SEM and SE^{2}LM methods. There are four sensors (TGS2602, TGS2620, and TGS2201A/B), all the sensors have similar trends when exposed to abnormal odors as shown in Fig. 4. The abnormal odor region recognition results for different methods are shown in Fig. 8, in which the rectangular windows are represented as detected abnormal odor regions (i.e., disturbance). Totally, four actual regions of abnormal

This article has been accepted for inclusion in a future issue of this journal. Content is final as presented, with the exception of pagination.

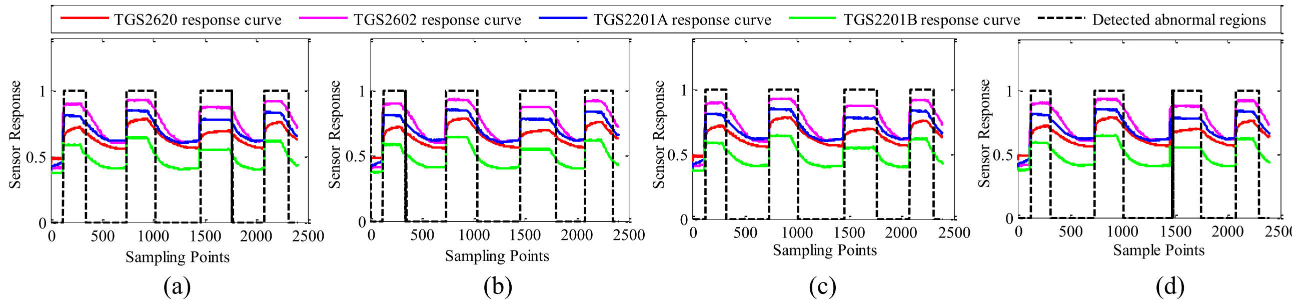

Fig. 8. Detected abnormal regions based on dataset 2. (a) SEM-sparse. (b) SEM-smooth. (c) SE^{2}LM (sigmoid). (d) SE^{2}LM (Gaussian).

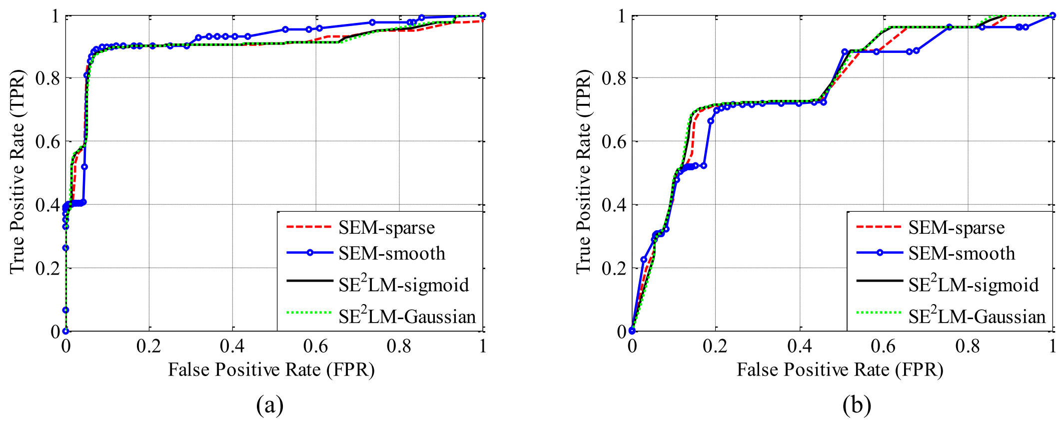

Fig. 9. ROC curves on real-time validation odor sequences. ROC curves on (a) dataset 2 and (b) dataset 3.

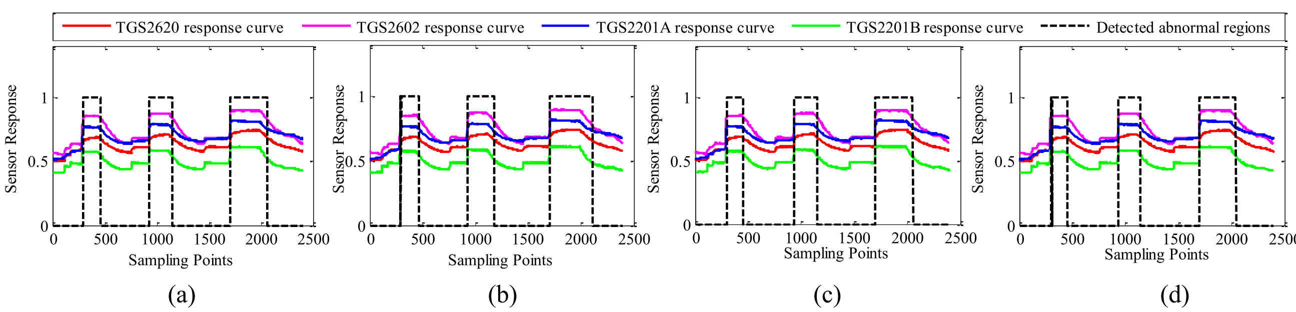

Fig. 10. Detected abnormal regions based on dataset 3. (a) SEM-sparse. (b) SEM-smooth. (c) SE^{2}LM (sigmoid). (d) SE^{2}LM (Gaussian).

odor with respect to Fig. 5 are correctly recognized. In addition to the qualitative recognition of regions, we have described the receiver operating characteristic curve (ROC) on this validation dataset 2 in Fig. 9(a), by computing true positive rate and false positive rate by adjusting the threshold T.

D. Validation on Real-Time Sequence Based on Dataset 3

This dataset is also real-time sequence in which the target odor also appears in experiment (as shown in Fig. 6), which is different from dataset 2. The abnormal odor region recognition results for different methods are shown in Fig. 10, where the regions labeled by rectangular windows are indicated as abnormal odor regions. The effectiveness of the proposed methods is clearly demonstrated. The ROC curves are shown in Fig. 9(b), and it shows that SE^{2}LM is better.

Note that, in the research area, there is very limited research work in abnormal odor detection. Therefore, the comparisons are conducted with the closely related work [20], [30], [31], in this paper. The superiority of the proposed methods is shown.

VI. Discussion

The key idea behind the proposed methods is to construct an internal relationship (i.e., self-correspondence) based on target odor data, such that the abnormal odor (i.e., disturbance) can be detected if only the established relationship is violated. The rationality and motivation behind are that it is hard and even impossible to collect all kinds of abnormal odors (countless) in real-world application scenarios by using an E-nose system. That is, the detection of abnormal odors cannot be simply recognized to be a binary classification problem. Therefore, we have to rely on the known prior knowledge of the target odors and establish a self-correspondence. During the compared methods, the PMIE method [31] actually relies on a regression idea, which attempts to construct

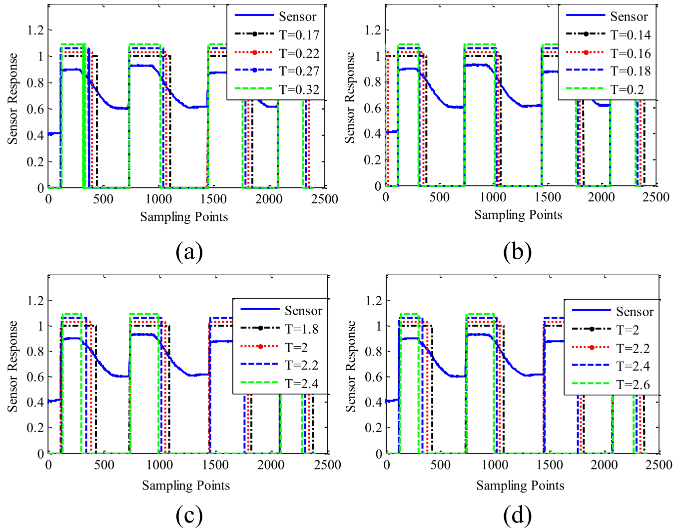

Fig. 11. Recognition on dataset 2 using different near-optimal T values. (a) SEM-sparse. (b) SEM-smooth. (c) SE^{2}LM (sigmoid). (d) SE^{2}LM (Gaussian).

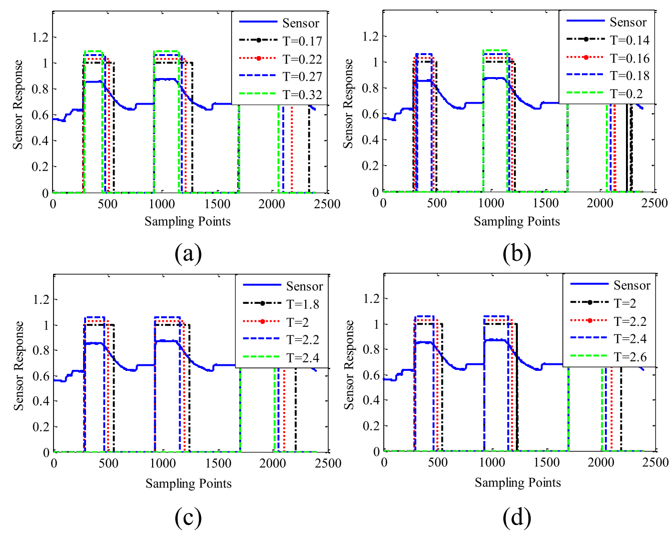

Fig. 12. Recognition on dataset 3 using different near-optimal T values. (a) SEM-sparse. (b) SEM-smooth. (c) SE^{2}LM (sigmoid). (d) SE^{2}LM (Gaussian).

a similar self-correspondence between sensors (i.e., five sensors are used to approximate the remaining one sensor for target odors), but neglect the property of internal independence assumption between sensors. In our methods, also, a very necessary step is to search an optimal violation threshold T (i.e., an appropriate decision bound). Actually, the value of bound T is important to decide rejection rate or acceptance rate of an unknown odor, which is also an important and difficult problem in machine learning. In this paper, we have discussed and presented the performance based on different T-values around the near-optimal T in rectangle window as shown in Fig. 7 for datasets 2 and 3, respectively. Specifically, we have selected four different T-values around the near-optimal T, and shown the recognized abnormal odor regions in datasets 2 and 3. The abnormal odor region detection results on both validation datasets based on different T-values are shown in Figs. 11 and 12, respectively. We observe that with the increasing of T value, the detected region is shrinking. That is, manual intervention can be made on the determination of the optimal T instead of the near-optimal T, due to its task-specific characteristic.

VII. Conclusion

In this paper, we focus on the challenge of abnormal odor detection (i.e., disturbance) in E-nose community. With our fabricated E-nose system, we propose two frameworks such as SEM and SE^{2}LM for abnormal odor detection, which consist of two general phases: 1) self-correspondence establishment (i.e., self-expression $\boldsymbol{\alpha}$) and 2) violation threshold T search. The strength of the proposed methods are twofold: 1) the self-correspondence α is easily implemented by using target odor data as invariant information and 2) the search of violation threshold T is conducted by using a very few abnormal odor data as prior knowledge, without considering countless kinds of abnormal odors in surroundings. The weakness of the proposed method lies in that the boundary of the abnormal odor regions may not be accurately estimated, due to the fuzzy sensor sensitivity problem. Numerous experiments by using our E-nose system were conducted, and the results demonstrate the effectiveness of the proposed methods. Particularly, in comparisons, the SE^{2}LM method shows a superior performance in real application scenarios. In our future work, we would address detection of mixtures, which is still an open problem in E-nose community. Also, the proposed method is implemented off-line, thus on-line representation of $\boldsymbol{\alpha}$ is necessary.

Acknowledgment

The authors would like to thank the Guest Editors and the anonymous reviewers for their insightful comments and concerns in the near future.

References

[1] K. Persaud and G. Dodd, "Analysis of discrimination mechanisms in the mammalian olfactory system using a model nose," *Nature*, vol. 299, pp. 352–355, Sep. 1982.

[2] J. W. Gardner and P. N. Bartlett, "A brief history of electronic noses," *Sensors Actuators B Chem.*, vols. 18–19, nos. 1–3, pp. 210–211, Mar. 1994.

[3] K. Brudzewski, S. Osowski, and T. Markiewicz, "Classification of milk by means of an electronic nose and SVM neural network," *Sensors Actuators B Chem.*, vol. 98, nos. 2–3, pp. 291–298, 2004.

[4] N. Bhattacharyya *et al.*, "Electronic nose for black tea classification and correlation of measurements with 'tea taster' marks," *IEEE Trans. Instrum. Meas.*, vol. 57, no. 7, pp. 1313–1321, Jul. 2008.

[5] M. Ghasemi-Varnamkhasti *et al.*, "Aging fingerprint characterization of beer using electronic nose," *Sensors Actuators B Chem.*, vol. 159, no. 1, pp. 51–59, Nov. 2011.

[6] L. Zhang *et al.*, "Classification of multiple indoor air contaminants by an electronic nose and a hybrid support vector machine," *Sensors Actuators B Chem.*, vol. 174, pp. 114–125, Nov. 2012.

[7] L. Dang *et al.*, "A novel classifier ensemble for recognition of multiple indoor air contaminants by an electronic nose," *Sensors Actuators A Phys.*, vol. 207, pp. 67–74, Mar. 2014.

[8] L. Zhang *et al.*, "Gases concentration estimation using heuristics and bio-inspired optimization models for experimental chemical electronic nose," *Sensors Actuators B Chem.*, vol. 160, no. 1, pp. 760–770, 2011.

[9] L. Zhang and F. Tian, "Performance study of multilayer perceptrons in a low-cost electronic nose," *IEEE Trans. Instrum. Meas.*, vol. 63, no. 7, pp. 1670–1679, Jul. 2014.

[10] A. D. Kenyon, V. M. Catterson, S. D. J. McArthur, and J. Twiddle, "An agent-based implementation of hidden Markov models for gas turbine condition monitoring," *IEEE Trans. Syst., Man, Cybern., Syst.*, vol. 44, no. 2, pp. 186–195, Feb. 2014.

[11] A. D'Amico *et al.*, "Olfactory systems for medical applications," *Sensors Actuators B Chem.*, vol. 130, no. 1, pp. 458–465, 2008.

[12] K. Yan, D. Zhang, D. Wu, H. Wei, and G. Lu, "Design of a breath analysis system for diabetes screening and blood glucose level prediction," *IEEE Trans. Biomed. Eng.*, vol. 61, no. 11, pp. 2787–2795, Nov. 2014.

[13] C. Di Natale *et al.*, "Lung cancer identification by the analysis of breath by means of an array of non-selective gas sensors," *Biosensors Bioelectron.*, vol. 18, no. 10, pp. 1209–1218, 2003.

[14] K. Brudzewski, S. Osowski, and A. Golembiecka, "Differential electronic nose and support vector machine for fast recognition of tobacco," *Expert Syst. Appl.*, vol. 39, no. 10, pp. 9886–9891, 2012.

[15] K. Brudzewski, S. Osowski, and W. Pawlowski, "Metal oxide sensor arrays for detection of explosives at sub-parts-per million concentration levels by the differential electronic nose," *Sensors Actuators B Chem.*, vol. 161, no. 1, pp. 528–533, 2012.

[16] I. Rodriguez-Lujan, J. Fonollosa, A. Vergara, M. Homer, and R. Huerta, "On the calibration of sensor arrays for pattern recognition using the minimal number of experiments," *Chemometrics Intell. Lab. Syst.*, vol. 130, pp. 123–134, Jan. 2014.

[17] X. Yin, L. Zhang, F. Tian, and D. Zhang, "Temperature modulated gas sensing E-nose system for low-cost and fast detection," *IEEE Sensors J.*, vol. 16, no. 2, pp. 464–474, Jan. 2016.

[18] R. Gosangi and R. Gutierrez-Osuna, "Active temperature programming for metal-oxide chemoresistors," *IEEE Sensors J.*, vol. 10, no. 6, pp. 1075–1082, Jun. 2010.

[19] S. K. Jha and K. Hayashi, "A novel odor filtering and sensing system combined with regression analysis for chemical vapor quantification," *Sensors Actuators B Chem.*, vol. 200, pp. 269–287, Sep. 2014.

[20] L. Zhang and D. Zhang, "Efficient solutions for discreteness, drift, and disturbance (3D) in electronic olfaction," *IEEE Trans. Syst., Man, Cybern., Syst.*, to be published, doi: 10.1109/TSMC.2016.2597800.

[21] K. Yan and D. Zhang, "Calibration transfer and drift compensation of e-noses via coupled task learning," *Sensors Actuators B Chem.*, vol. 225, pp. 288–297, Mar. 2016.

[22] L. Zhang, F.-C. Tian, X.-W. Peng, and X. Yin, "A rapid discreteness correction scheme for reproducibility enhancement among a batch of MOS gas sensors," *Sensors Actuators A Phys.*, vol. 205, pp. 170–176, Jan. 2014.

[23] J. Fonollosa, L. Fernández, A. Gutiérrez-Gálvez, R. Huerta, and S. Marco, "Calibration transfer and drift counteraction in chemical sensor arrays using direct standardization," *Sensors Actuators B Chem.*, vol. 236, pp. 1044–1053, Nov. 2016.

[24] L. Zhang *et al.*, "On-line sensor calibration transfer among electronic nose instruments for monitoring volatile organic chemicals in indoor air quality," *Sensors Actuators B Chem.*, vol. 160, no. 1, pp. 899–909, 2011.

[25] M. Padilla *et al.*, "Drift compensation of gas sensor array data by orthogonal signal correction," *Chemometrics Intell. Lab. Syst.*, vol. 100, no. 1, pp. 28–35, 2010.

[26] A. Ziyatdinov *et al.*, "Drift compensation of gas sensor array data by common principal component analysis," *Sensors Actuators B Chem.*, vol. 146, no. 2, pp. 460–465, Apr. 2010.

[27] H. Ding, L. Jun-hua, and S. Zhong-Ru, "Drift reduction of gas sensor by wavelet and principal component analysis," *Sensors Actuators B Chem.*, vol. 96, nos. 1–2, pp. 354–363, Nov. 2003.

[28] L. Zhang and D. Zhang, "Domain adaptation extreme learning machines for drift compensation in E-nose systems," *IEEE Trans. Instrum. Meas.*, vol. 64, no. 7, pp. 1790–1801, Jul. 2015.

[29] K. Yan and D. Zhang, "Correcting instrumental variation and time-varying drift: A transfer learning approach with autoencoders," *IEEE Trans. Instrum. Meas.*, vol. 65, no. 9, pp. 2012–2022, Sep. 2016.

[30] L. Zhang *et al.*, "A novel background interferences elimination method in electronic nose using pattern recognition," *Sensors Actuators A Phys.*, vol. 201, pp. 254–263, Oct. 2013.

[31] F. Tian, Z. Liang, L. Zhang, Y. Liu, and Z. Zhao, "A novel pattern mismatch based interference elimination technique in E-nose," *Sensors Actuators B Chem.*, vol. 234, pp. 703–712, Oct. 2016.

[32] G.-B. Huang, Q.-Y. Zhu, and C.-K. Siew, "Extreme learning machine: Theory and applications," *Neurocomputing*, vol. 70, nos. 1–3, pp. 489–501, 2006.

[33] G.-B. Huang, H. Zhou, X. Ding, and R. Zhang, "Extreme learning machine for regression and multiclass classification," *IEEE Trans. Syst., Man, Cybern. B, Cybern.*, vol. 42, no. 2, pp. 513–529, Apr. 2012.

[34] J. Tang, C. Deng, and G.-B. Huang, "Extreme learning machine for multilayer perceptron," *IEEE Trans. Neural Netw. Learn. Syst.*, vol. 27, no. 4, pp. 809–821, Apr. 2015.

[35] L. Zhang and D. Zhang, "Robust visual knowledge transfer via extreme learning machine-based domain adaptation," *IEEE Trans. Image Process.*, vol. 25, no. 10, pp. 4959–4973, Oct. 2016, doi: 10.1109/TIP.2016.2598679.

[36] G.-B. Huang, Z. Bai, L. L. C. Kasun, and C. M. Vong, "Local receptive fields based extreme learning machine," *IEEE Commun. Mag.*, vol. 10, no. 2, pp. 18–29, May 2015.

[37] G.-B. Huang, "What are extreme learning machines? Filling the gap between frank Rosenblatt's dream and John von Neumann's puzzle," *Cogn. Comput.*, vol. 7, no. 3, pp. 263–278, 2015.

[38] G.-B. Huang, "An insight into extreme learning machines: Random neurons, random features and kernels," *Cogn. Comput.*, vol. 6, no. 3, pp. 376–390, 2014.

[39] F. Sun, C. Liu, W. Huang, and J. Zhang, "Object classification and grasp planning using visual and tactile sensing," *IEEE Trans. Syst., Man, Cybern., Syst.*, vol. 46, no. 7, pp. 969–979, Jul. 2016.

[40] H. Kaindl, M. Vallee, and E. Arnautovic, "Self-representation for self-configuration and monitoring in agent-based flexible automation systems," *IEEE Trans. Syst., Man, Cybern., Syst.*, vol. 43, no. 1, pp. 164–175, Jan. 2013.

[41] V. Bruni and D. Vitulano, "An improvement of kernel-based object tracking based on human perception," *IEEE Trans. Syst., Man, Cybern., Syst.*, vol. 44, no. 11, pp. 1474–1485, Nov. 2014.

[42] Ç. Aytekin, Y. Rezaeitabar, S. Dogru, and I. Ulusoy, "Railway fastener inspection by real-time machine vision," *IEEE Trans. Syst., Man, Cybern., Syst.*, vol. 45, no. 7, pp. 1101–1107, Jul. 2015.

[43] L. Zhang, W. M. Zuo, and D. Zhang, "LSDT: Latent sparse domain transfer learning for visual adaptation," *IEEE Trans. Image Process.*, vol. 25, no. 3, pp. 1177–1191, Mar. 2016.

[44] R. Tibshirani, "Regression shrinkage and selection via the lasso," *J. Roy. Stat. Soc. B*, vol. 58, no. 1, pp. 267–288, 1996.

[45] E. Phaisangittisagul and H. T. Nagle, "Enhancing multiple classifier system performance for machine olfaction using odor-type signatures," *Sensors Actuators B Chem.*, vol. 125, no. 1, pp. 246–253, 2007.

Lei Zhang (M'14) received the Ph.D. degree in circuits and systems from the College of Communication Engineering, Chongqing University, Chongqing, China, in 2013.

He is currently a Professor/Distinguished Research Fellow with Chongqing University. He was selected as a Hong Kong Scholar in China in 2013. He was a Post-Doctoral Fellow with Hong Kong Polytechnic University, Hong Kong, from 2013 to 2015. He has authored over 50 scientific papers in top journals, including several IEEE TRANSACTIONS, such as the IEEE TRANSACTIONS ON NEURAL NETWORKS AND LEARNING SYSTEMS, the IEEE TRANSACTIONS ON IMAGE PROCESSING, the IEEE TRANSACTIONS ON MULTIMEDIA, the IEEE TRANSACTIONS ON INSTRUMENTATION AND MEASUREMENT, the IEEE TRANSACTIONS ON SYSTEMS, MAN, AND CYBERNETICS—PART A: SYSTEMS AND HUMANS, the IEEE SENSORS JOURNAL, *Information Fusion*, *Sensors and Actuators B*, and *Analytica Chimica Acta*. His current research interests include machine learning, pattern recognition, electronic olfaction, computer vision, and multisensor system.

Dr. Zhang was a recipient of the Outstanding Doctoral Dissertation Award of Chongqing, China, in 2015, the Hong Kong Scholar Award in 2014, the Academy Award for Youth Innovation of Chongqing University in 2013, and the New Academic Researcher Award for Doctoral Candidates from the Ministry of Education, China, in 2012.

Pingling Deng received the bachelor's degree in information science and engineering from Lanzhou University, Lanzhou, China, in 2015. She is currently pursuing the M.Sc. degree with Chongqing University, Chongqing, China.

Her current research interests include electronic nose and extreme learning machines.